ChemPhotoChem

Research Articles
doi.org/10.1002/cptc.202200152

Chemistry Europe
European Chemical Societies Publishing

www.chemphotochem.org

Orthogonal- and Path-Dependent Photo/Acidoswitching in an Eight-State Dihydroazulene-Spiropyran Dyad

Mathias Dowds,[a] Stine G. Stenspil,[a] João H. de Souza,[a] Bo W. Laursen,[a] Martina Cacciarini,*[b] and Mogens Brøndsted Nielsen*[a]

Molecules comprised of two or more switches have potential to exist in a variety of states, which may only be accessible by a "correct" sequence of stimuli on account of the influence of the neighboring unit. Here we present a straightforward synthesis of a dyad incorporating two photoswitchable units, dihydroazulene (DHA) and spiropyran (SP). The photoswitching properties of both chromophores and the acido-triggered switching of the SP were retained in the dyad, allowing selective switching between eight states with distinct absorption and fluorescence properties (corresponding to light-controlled fluorescence on/off switching). Photoisomerization of DHA and protonation of SP allowed an orthogonal control of the individual sites. Conversely, photoisomerization of SP to its merocyanine (MC) isomer could not be performed without also addressing DHA-to-vinylheptafulvene (VHF) switching. Access to the **DHA-MC** state thus appeared to be path-dependent as it could exclusively be reached by deprotonation of the thermally stable **DHA-*E*-MCH**.

Introduction

Molecular switches are molecules that are able to undergo reversible transformations between at least two (meta-) stable states in response to external stimuli and therefore are associated to binary number systems.[1] Photochromic molecules are photoswitches and experience great attention due to the possibility of precisely controlling the applied light stimulus in terms of space and energy. As a consequence, they have been key components of molecular motors and machines,[2–6] in photocontrolled biological systems and materials,[7–10] thermoprobes,[11] molecular electronics devices,[12] adhesives,[13] and energy storage systems.[14–16] Commonly used photochromic systems are based on *cis/trans* isomerizations of azobenzenes,[14] or alkenes[2,17,18] (e.g. in combination with atropisomerism as recently reported[19]) or ring-opening/closure reactions in dithienylethenes,[20] norbornadienes,[15] dihydroazulenes,[16] or spiropyrans.[8]

Most photoswitches alternate reversibly between two distinct states upon irradiation with light. Combining multiple photochromic units of either the same[21–24] or different[25–28] types in one molecule allows for development of complex switchable structures enhancing the number of possible switching states.[29] Thereby, eight states were for example reached in an unsymmetrical system with two photoswitchable sites and one acidoswitchable one,[30] and a symmetrical system consisting of four photoswitchable units showed nine-state multichromism.[24]

Depending on the orthogonality of the switching stimuli, access to one (or multiple) specific state(s) may become path-dependent. Figure 1 illustrates possible switching schemes for a hypothetical system with two switchable sites. The four

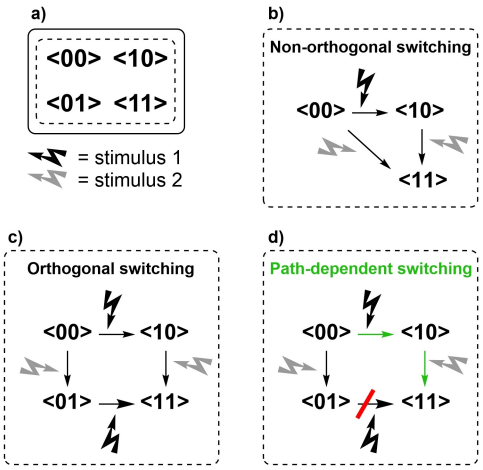

Figure 1. Stimuli-dependent switching in a system with two switching sites. **a**) Binary code for the four possible states. **b**) Non-orthogonal switching: stimulus 1 affects one site; stimulus 2 affects both sites, rendering the <01> state inaccessible. **c**) Orthogonal switching: the stimuli affect different sites; all states are accessible. State <11> can be reached via both <01> and <10>. **d**) Path-dependent switching: one state, here <11>, can only be accessed via one specific pathway (green arrows).

[a] *Dr. M. Dowds, S. G. Stenspil, J. H. de Souza, Prof. Dr. B. W. Laursen, Prof. Dr. M. B. Nielsen*
Department of Chemistry
University of Copenhagen
Universitetsparken 5, 2100 Copenhagen Ø (Denmark)
E-mail: mbn@chem.ku.dk
[b] *Prof. Dr. M. Cacciarini*
Department of Chemistry
University of Florence
via della Lastruccia 3–13, 50019 Sesto Fiorentino (Italy)
E-mail: martina.cacciarini@unifi.it

Supporting information for this article is available on the WWW under https://doi.org/10.1002/cptc.202200152

switching states can be described by binary code: <00>, <10>, <01>, <11> (Figure 1a). In the case of non-orthogonal switching (Figure 1b), the first stimulus switches the one site, while the other remains inert (<00> → <10>). The second stimulus induces switching of both sites, thus rendering the <01> state inaccessible. The <01> state becomes accessible by orthogonal switching as shown in Figure 1c; i.e. each stimulus affects one site, but not the other. In the case of path-dependent switching, all four states can be accessed selectively, but the state <11> can only be reached from one specific sequence of stimuli (one pathway) as illustrated in Figure 1d. In this work, we present a dyad system that contains both concepts of orthogonality and path-dependency.

2-Phenyl-1,1,-dicyano-1,8*a*-dihydroazulene (**DHA**) and its derivatives undergo ring-opening upon irradiation (λ = 350–420 nm), forming the vinylheptafulvene (**VHF**) isomer (Scheme 1a).[31,32] This isomerization is accompanied by a change in dipole moments and in longest-wavelength absorption maximum from 353 nm (**DHA**) to 470 nm (**VHF**) in MeCN. Moreover, in contrast to **VHF**, **DHA** shows some minor fluorescence (quantum yield of 0.03% in EtOH at 24 °C) with an emission maximum at 460 nm.[31] The VHF-to-DHA back-reaction is not light-activated, but occurs thermally with a half-life of 218 min at 25 °C in MeCN.[32]

Spiropyran (**SP**) also undergoes ring-opening when irradiated with UV light (Scheme 1b). The formation of a merocyanine (**MC**) is accompanied by large changes in several properties, such as dipole moments, dielectric constants, and geometrical dimensions.[8] The extended π-conjugation results in **MC** absorbing in the visible region ($\lambda_{max,abs}$ = 550–600 nm) and exhibiting red emission ($\lambda_{max,em}$ = ca. 650 nm).[8,33] The back-reaction from **MC** to **SP** is thermally reversible and can be accelerated by irradiation with visible light. The addition of acid to **SP** results in ring-opening of the spiropyran and formation of protonated merocyanine in its *Z* configuration (***Z*-MCH**), which thermally relaxes to the respective *E* isomer ***E*-MCH** ($\lambda_{max,abs}$ = ca. 420 nm).[33–36] Protonation of **MC** in the photostationary state yields ***E*-MCH** directly.[33–35] Both ***Z*-MCH** and ***E*-MCH** can be deprotonated to yield **SP** and **MC**, respectively.[33,34]

We became interested to explore how DHA and SP units influence each other's optical and switching properties when connected. In this work, we present the synthesis and characterization of the dyad **DHA-SP** (Scheme 2), and we show how to uniquely access several isomerizations of this multimodal system. With the two switching states of the dihydroazulene moiety (DHA and VHF), and four states of the spiropyran unit (SP, MC, *Z*-MCH, *E*-MCH), eight different switching states of this dyad are theoretically possible (ignoring stereoisomers). In other words, the dyad can be described as a combination of three switching dimensions, from 000 to 111 in binary code. Of these eight states, two – **DHA-SP** and **DHA-*E*-MCH** (Scheme 3) – should form a bistable pair and the other six states should relax thermally to one of these two states. In binary code, the first digit can represent the switching state of the DHA moiety (0 = DHA, 1 = VHF) and the subsequent two digits represent the switching state of the SP moiety. Thus, the second digit represents the configuration of the ethylene bridge in SP and *Z*-MCH (0) versus MC and *E*-MCH (1). The third digit represents the neutral (0, SP or MC) versus the protonated (1, *Z*-MCH or *E*-MCH) species of the spiropyran moiety (Scheme 1). Gratifyingly, careful modulation of light/heat and acid/base stimuli allowed interchanging among all these eight different forms based on

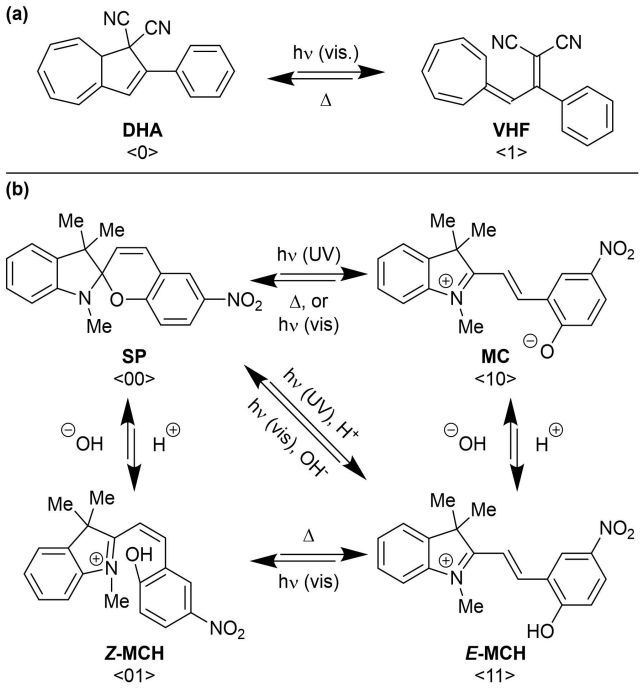

Scheme 1. General switching behavior of (a) dihydroazulene (**DHA**)/vinylheptafulvene (**VHF**) and (b) spiropyran (**SP**)/merocyanine (**MC**)/protonated *Z*-merocyanine (***Z*-MCH**)/protonated *E*-merocyanine (***E*-MCH**). The equivalent binary code represents each switching state of dihydroazulene and spiropyran, respectively.

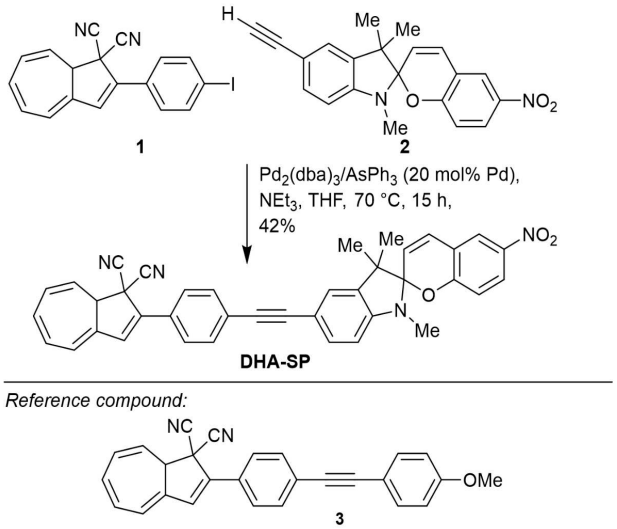

Scheme 2. Top: Synthesis of **DHA-SP** from the precursors **1** and **2** *via* a Sonogashira coupling. **Bottom**: DHA **3** was synthesized from **1** as a reference compound for UV-vis absorption and fluorescence measurements.

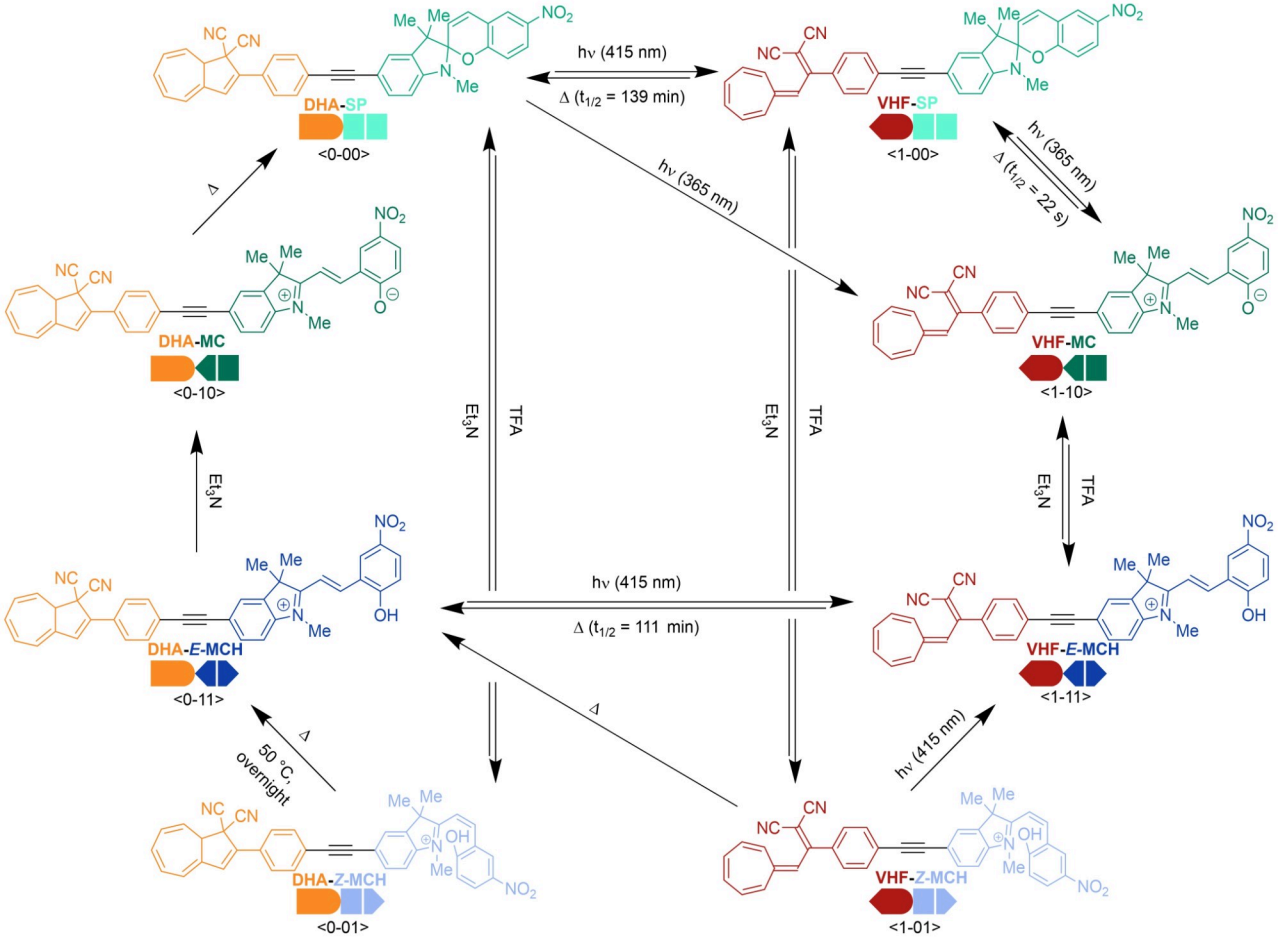

Scheme 3. Overview of the observed photo-, acid-, and base-induced switching reactions and the thermal relaxations of the eight states of the dyad. TFA: Trifluoroacetic acid. Solvent: acetonitrile.

NMR and UV-Vis absorption spectroscopic studies. Moreover, the emissive properties of the merocyanine allowed us to use fluorescence as an additional readout channel.

Results and Discussion

Synthesis

The synthesis of the dyad **DHA-SP** from the precursors **1**[37] and **2**[38] (prepared according to literature) was carried out under Sonogashira coupling conditions (Scheme 2). When using Pd^{II}/Cu^{I} as catalyst system, we observed high conversions of **1** and **2**, but also substantial amounts of homocoupling of the acetylenic spiropyran **2** into a butadiyne product. Removing this resulting side product via repeated column chromatography reduced the isolated yield of **DHA-SP** below 10%. It was nevertheless possible to suppress the homocoupling by using tris(dibenzylideneacetone)dipalladium(0) and triphenyl arsine as catalyst system, and thereby **DHA-SP** was isolated in 42% yield.

Photoswitching Properties

The switching reactions of the dyad were studied by ^{1}H NMR and UV-Vis absorption spectroscopies and are summarized in Scheme 3. The DHA unit underwent photoisomerization upon irradiation with 365 nm or 415 nm light, whereas the formation of the MC unit from the SP unit occurred only upon irradiation with 365 nm light. Therefore, **DHA-SP** can selectively be photoisomerized to **VHF-SP**. As irradiation with 365 nm light induced photoswitching of both DHA and SP, **VHF-MC** is the only photo-accessible state that contains MC. The SP units of **DHA-SP** and **VHF-SP** can be protonated by trifluoroacetic acid (TFA), yielding the **DHA-*Z*-MCH** and **VHF-*Z*-MCH**, respectively. The **DHA-*Z*-MCH** subsequently transformed into **DHA-*E*-MCH**. In **VHF-*Z*-MCH**, the thermal conversion of *Z*-MCH to *E*-MCH is accompanied by thermal ring-closing of VHF to DHA, giving **DHA-*E*-MCH**. Irradiating **VHF-*Z*-MCH** or **DHA-*E*-MCH** with UV or visible light (365 or 415 nm) yielded **VHF-*E*-MCH**, which could also be accessed by addition of TFA to **VHF-MC**.

The VHF-to-DHA and MC-to-SP back-reactions occurred spontaneously at 25 °C, whereas *E*-MCH was found to be stable. When deprotonated by triethylamine, **DHA-*Z*-MCH** and **VHF-*Z*-MCH** yielded **DHA-SP** and **VHF-SP**, respectively. The deprotona-

tion of **DHA-*E*-MCH** and **VHF-*E*-MCH** generated **DHA-MC** and **VHF-MC**, which both underwent fast relaxation to their respective SP isomers. Therefore, **DHA-MC** and **VHF-MC** could only be investigated by UV-vis absorption spectroscopy. **DHA-MC** could only be accessed *via* deprotonation of **DHA-*E*-MCH** (corresponding to path-dependent switching).

Thus, the three states **DHA-*Z*-MCH** (<001>), **VHF-SP** (<100>), and **VHF-*Z*-MCH** (<101>) could be accessed orthogonally starting from **DHA-SP** (<000>). The Z-MCH isomers acted as intermediate to reach **DHA-*E*-MCH** (<011>) by thermal relaxation at 50 °C overnight. State **VHF-*E*-MCH** (<111>) could be obtained by photoisomerization of **DHA-*E*-MCH** (<011>) or of **VHF-*Z*-MCH** (<101>), or by protonation of **VHF-MC** (<110>). The combination of bidirectional switching between SP and *Z*-MCH and unidirectional thermal relaxation to *E*-MCH allowed us to obtain **DHA-*E*-MCH** (<011>) *via* three possible paths starting from **DHA-SP** (<000>): a) protonation followed by thermal relaxation (*via* **DHA-*Z*-MCH**/<001>); b) irradiation with 415 nm light, followed by protonation and thermal relaxation (*via* **VHF-SP**/<100> and **VHF-*Z*-MCH**/<101>); or c) irradiation with 365 nm light followed by protonation and relaxation (*via* **VHF-MC**/<110> and **VHF-*E*-MCH**/<111>). Simultaneously, **VHF-*E*-MCH** could be obtained following three sequences with either **DHA-*E*-MCH** (<011>), **VHF-MC** (<110>), or **VHF-*Z*-MCH** (<101>) as key intermediates. **DHA-*E*-MCH** (<011>) acted as starting point for the only route to access **DHA-MC** (<010>): deprotonation of the *E*-MCH unit resulted in formation of **DHA-MC** (<010>), which quickly relaxed to **DHA-SP** (<000>).

^{1}H NMR Spectroscopy

Six distinct states of switching could be detected by ^{1}H NMR spectroscopy (Figure 2, symbols highlight distinctive signals for each switching state). As for **DHA-SP** (Figure 2a), the singlet at 7.20 ppm can be assigned to the DHA 3-position, while a ddd at 6.35 ppm and a dd at 5.83 ppm are assigned to the protons at the DHA 7- and 8-positions, respectively. Changing the switching state of the spiropyran site by protonation to **DHA-*Z*-MCH** and subsequent opening to **DHA-*E*-MCH** (Figures 2b and 2c, respectively) barely influences the DHA signals. The signals of the DHA 7- and 8-positions exhibit no shielding or deshielding as compared to DHA-SP. The singlet of the DHA-3 position was mildly deshielded by 0.02 ppm in both, **DHA-*Z*-MCH** and **DHA-*E*-MCH**.

Upon irradiation with 415 nm light, the DHA resonances vanished and signals corresponding to VHF units appeared in **VHF-SP** (Figure 2d). The signal corresponding to the 3-proton was shielded from 7.20 ppm in DHA to 6.31 ppm in VHF, whereas the protons in the 7-membered ring experienced overall deshielding. The doublet of triplets with a shift of

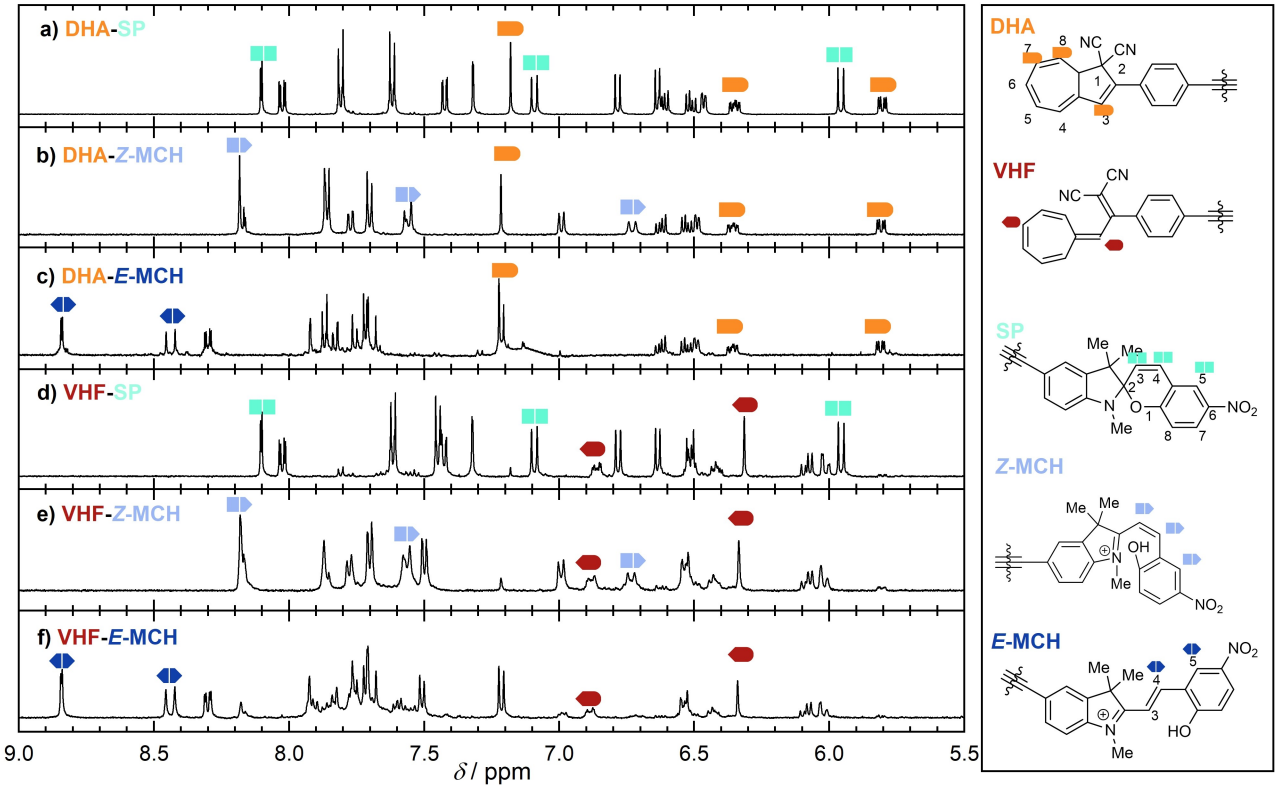

Figure 2. Left: Aromatic region of ^{1}H NMR spectra of (top to bottom): **DHA-SP**, **DHA-*Z*-MCH**, **DHA-*E*-MCH**, **VHF-SP**, **VHF-*Z*-MCH**, and **VHF-*E*-MCH** in CD_3CN. The labelled signals correspond to characteristic protons of each switchable moiety. **Right**: Structures of the DHA, VHF, SP, *Z*-MCH, and *E*-MCH moieties; the characteristic protons are labelled.

6.86 ppm is indicative for the VHF state. Similar to the DHA resonances, the chemical shifts of the VHF protons are almost independent from the switching state of the spiropyran side. All VHF signals experience a deshielding of ca. 0.02 ppm in **VHF-*Z*-MCH** (Figure 2e) and **VHF-*E*-MCH** (Figure 2f) as compared to **VHF-SP**.

The proton resonances of the chromene moiety are most indicative for the switching state of the SP unit. With a coupling constant of 10.4 Hz and chemical shifts of 7.09 and 5.95 ppm in **DHA-SP**, the doublets corresponding to the protons 3 and 4 in the ethylene bridge in the SP moiety are indicative of the SP state (Figure 2a). Additionally, the proton at the 5-position *ortho* to the bridge is especially distinctive and exhibits the strongest deshielding with a chemical shift of 8.10 ppm. These three resonances are also found in the spectrum of **VHF-SP** (Figure 2d).

Notably, the protonation of **DHA-SP** and **VHF-SP** with 50 equiv. of TFA did not immediately yield the *E*-MCH. Instead, we observed significant deshielding of the doublets corresponding to the 3- and 4-positions in SP and *Z*-MCH by 0.77 and 0.45 ppm. However, the methyl groups at the indole's 3-postion appear as one singlet in **DHA-*Z*-MCH** and **VHF-*Z*-MCH**, proving the loss of the stereogenic spiro center upon ring opening (see SI, chapter 6). Additionally, the coupling constant increased to 12.5 Hz, still indicating a *Z*-configuration of the double bond. Subsequently, we were able to obtain pure **DHA-*E*-MCH** after thermal *Z/E* isomerization of the **DHA-*Z*-MCH** merocyanine's double bond. The most obvious change as compared to the spectrum of **DHA-*Z*-MCH** is the further deshielding of the 4-proton to 8.44 ppm and a change of the coupling constant to 16.5 Hz, clearly indicating an *E* configuration of the double bond. The 3-proton was deshielded to ca. 7.5 ppm, but the signal is overlaid by DHA signals (or VHF signals in case of **VHF-*E*-MCH**). Additionally, the 5-proton undergoes a deshielding to 8.87 ppm. Irradiation of **VHF-*Z*-MCH** with 415 nm light resulted in almost full conversion to **VHF-*E*-MCH**. The shifts of the *E*-MCH protons were independent from the switching state of the DHA side.

It was not possible to investigate either **DHA-MC** or **VHF-MC** by NMR spectroscopy due to fast MC-to-SP conversion (see SI, Figure S19 and S20). The formation of **DHA-MC** and **VHF-MC**, and their transformation into the respective SP species were, however, confirmed by UV-Vis absorption spectroscopy (*vide infra*, see Figure 3 for UV-Vis absorption spectra of all states).

UV-Vis Absorption Spectroscopy: In the absorption spectra of the different switching states (Figure 3), the main absorption bands agree well with individual states of the DHA/VHF and SP/MC/*Z*-MCH/*E*-MCH components (Scheme 3). The parent DHA units show a characteristic longest-wavelength absorption band at $\lambda_{max} \approx 355$ nm, which shifts to 380 nm in the reference compound **3-DHA** that was extended by a 4-methoxyphenylacetylene moiety (Figure 3). The further redshift of the first DHA absorption band to 390 nm in the **DHA-SP** dyad indicates that the absorbing chromophore includes the phenylacetylene moiety and the attached nitrogen donor group, which is formally part of the SP switch.

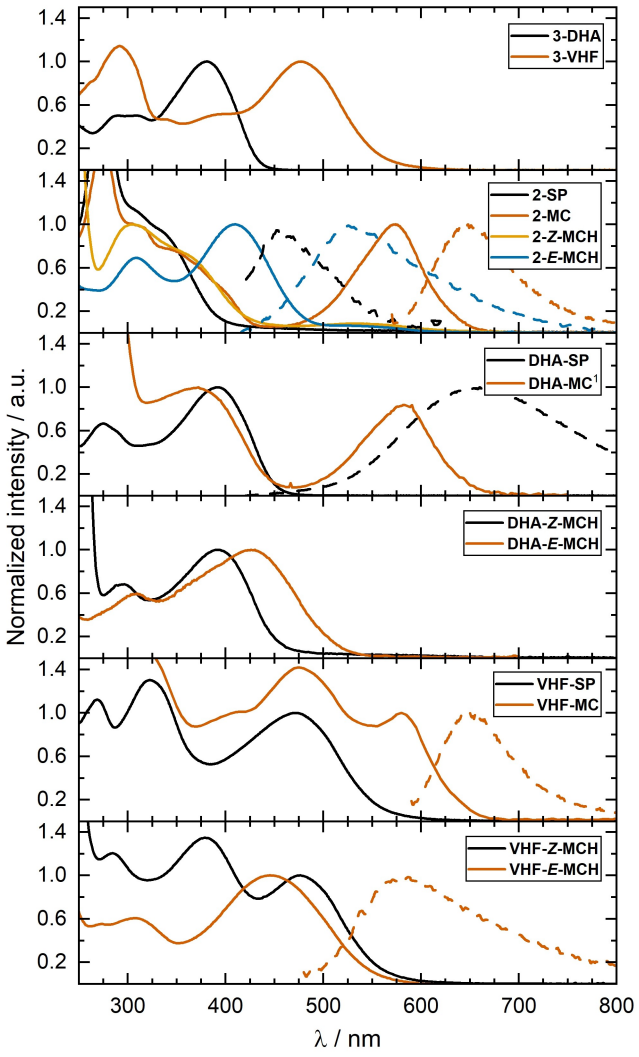

Figure 3. Normalized absorption (solid lines) and emission spectra (dashed lines) of **3-DHA**, **3-VHF**; **2-SP**, **2-MC**, **2-*Z*-MCH**, **2-*E*-MCH**; **DHA-SP**, **DHA-MC**; **DHA-*Z*-MCH**, **DHA-*E*-MCH**; **VHF-SP**, **VHF-MC**; **VHF-*Z*-MCH**, **VHF-*Z*-MCH** (top to bottom) in MeCN. Absorption spectra were normalized relative to the lowest-energy absorption band. [1]Obtained by addition of triethyl amine to **DHA-*E*-MCH**.

Switching of the DHA moieties to their VHF counterparts gave rise to a redshift of the first absorption band to 475 nm in the **VHF-SP**, **VHF-MC** configurations of the dyad as well as in **3-VHF** (Figure 3). Interestingly, the energy of this VHF absorption band is mostly independent of the phenylacetylene extension and is found at the same wavelength for the parent unsubstituted **VHF**, showing that the VHF chromophore is localized in the fundamental vinylheptafulvene unit. However, for the protonated **VHF-*E*-MCH**, a blueshift of the VHF band is observed, probably resulting from the electron deficient nature of the indole nitrogen.

Spiropyrans do only exhibit one characteristic UV absorption band at $\lambda_{max} \approx 270$ nm that was not significantly shifted in **DHA-SP** and **VHF-SP** as compared to **2-SP** (Figures S3, S6, and S10). Ring-opening to MC gives rise to a broad absorption in the visible region, which was also independent from the

substitution in **VHF-MC** and **2-MC** (λ_{max} = 580 and 574 nm, respectively). Protonation of the MC unit, to give *E*-MCH, drastically blueshifts this band to $\lambda_{max} \approx 420$ nm as a consequence of the reduced donor strength of the phenol compared to phenolate.

As **2-*Z*-MCH** is more blueshifted than **DHA-SP**, it follows that **DHA-*Z*-MCH** formed upon protonation did not result in any significant shift of the first absorption band compared to **DHA-SP**. **DHA-*E*-MCH** does redshift (λ_{max} = 421) in agreement with the position of the first absorption band of **2-*E*-MCH** (λ_{max} = 409 nm). The *E*-MCH absorption of **VHF-*E*-MCH** is not clearly distinct from the VHF absorption (λ_{max} = 471 nm). The thermal half-life of the back-reaction from **VHF-SP** to **DHA-SP** was determined to 139 min at 25 °C, which is virtually identical to the half-life of **3-VHF**. The thermal back-reaction of the VHF moiety was slightly accelerated (half-life of 111 min) by protonation of the SP unit to form **VHF-*E*-MCH**.[39] The faster VHF ring closure is the result of an increased electron-withdrawing influence of the *E*-MCH unit on the VHF relative to that exerted by the SP unit, in line with previous studies on simpler model systems.[40] The ethynyl substituent at the spiropyran's indoline moiety of **2** and **DHA-SP** induces a fast thermal MC-to-SP relaxation with half-lives of approx. 30 s for the **2-MC**-to-**2-SP** and **VHF-MC**-to-**VHF-SP** conversions. Due to the heat of neutralization after the addition of Et_3N to the solution of **DHA-*E*-MCH** and TFA in acetonitrile, the detected half-life of **DHA-MC** of ca. 20 s is not directly comparable to the other thermal relaxation. However, we were able to access **VHF-MC** also via deprotonation of **VHF-*E*-MCH** with Et_3N and detected a half-life of ca. 10 s. Thus, the DHA/VHF switching state exerts an influence on the MC/SP relaxation.

We obtained photoswitching quantum yields of only 5% for the formation of **VHF-SP** from **DHA-SP** and 1% for the formation of **VHF-*E*-MCH** from **DHA-*E*-MCH** upon irradiation at 415 nm in MeCN, while the parent **DHA**-to-**VHF** conversion has a quantum yield of 14% at 415 nm.[31]

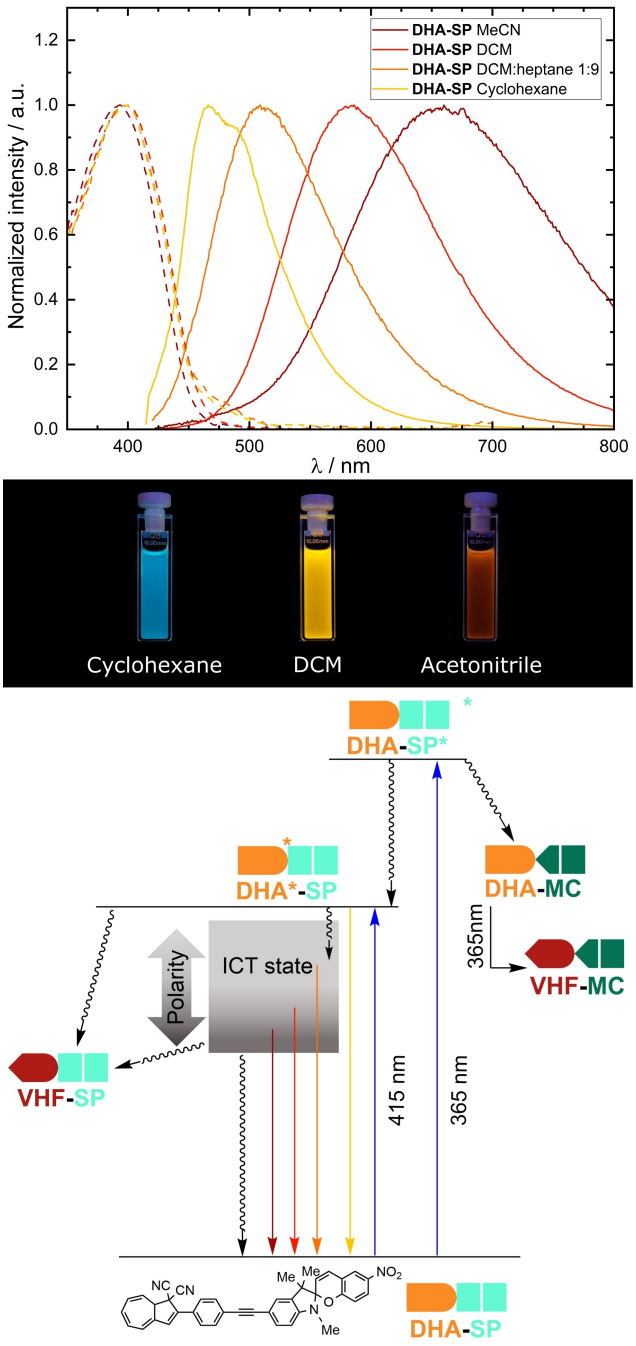

Figure 4. Top: Normalized absorption (dashed lines) and fluorescence (solid lines) of DHA-SP in MeCN, dichloromethane (DCM), DCM:heptane (1:9), and cyclohexane. **Middle**: Photographs of the fluorescence of DHA-SP solutions (c = 77 µmol/L) in cyclohexane, DCM and acetonitrile under UV irradiation (365 nm). **Bottom**: State diagram of **DHA-SP** outlining the main processes occurring after excitation by either 365 nm or 415 nm light. The energy of the ICT state is highly solvent dependent as indicated by the broad grey level and the different coloration of the emission arrows.

Fluorescence Spectroscopy

DHA-SP displays an unexpected, broad and highly redshifted emission with $\lambda_{f,max}$ at 660 nm in MeCN (Figure 4), corresponding to an extremely large Stokes shift of 10300 cm^{-1} ($\lambda_{abs,max}$ = 390 nm). Excitation spectra at multiple emission wavelengths superimposed well on the absorption spectrum confirming **DHA-SP** as the emitter (Figure S26). Individually, the parent compounds **VHF**[31] and **2-SP**[41–43] are practically non-fluorescent, while the **DHA** scaffold exhibits weak fluorescence with quantum yields below 0.1%.[31] Fluorescence does also occur from MC species with typical quantum yields of 1%.[44] However, these emissions of the MC species are widely different from the new emission observed for **DHA-SP**. The MC emission from both **2-MC** and **VHF-MC** has a maximum at 648 nm close to $\lambda_{f,max}$ of the **DHA-SP**. As these emission bands are much narrower and the Stokes shifts are not nearly as large (< 2000 cm^{-1}, in MeCN), we exclude MC as the origin of the **DHA-SP** emission. The protonated intermediates **DHA-*Z*-MCH** and **VHF-*Z*-MCH** are not emissive. **DHA-*E*-MCH** is non-fluorescent and the very weak fluorescence detected from the sample was assigned via excitation spectra to originate from residual **DHA-SP**. In its open form, **VHF-*E*-MCH** displays a new emission band similar in shape to that of **2-*E*-MCH** but redshifted probably due to the conjugation to VHF. The reference

compound **3-DHA** does not show fluorescence even though the absorbing chromophore bears close resemblance to **DHA-SP**. In **VHF-SP** – where the first absorption band clearly resembles the basic VHF chromophore – no emission is observed.

Investigation of solvent effect on the **DHA-SP** fluorescence, in cyclohexane, dichloromethane (DCM):heptane (1:9), DCM, and MeCN showed hardly any shifts in the absorption spectra, while the emission band underwent very large redshifts with increasing polarity of the solvent (Figure 4, top, and Table S4). Such large Stokes shifts and drastic solvent effects in the emission spectra are characteristic of chromophores with intramolecular charge transfer (ICT) states, where a rearrangement of the charges occurs in the excited state.[45] In cyclohexane, the Stokes shift is significantly reduced to $<3700\ cm^{-1}$ and some vibronic fine structure is observed indicating that the locally excited (LE) state may be contributing to the emission in this very low polarity solvent. The absence of solvatochromism in the absorption spectra supports the notation that there is little or no charge transfer character in the initially formed excited state and that the polar emissive ICT state is formed after excitation. ICT states are typically found in molecules that contain donor and acceptor groups to facilitate the polar ICT state. We suggest that the aniline unit in **DHA-SP** is the donor group and **DHA** the acceptor group. Similar large solvent response and Stokes shifts were observed for related 4-dimethylamino-diphenylacetylene systems carrying carbonyl or cyano acceptors in the 4′ position.[46] The fluorescence behavior of DHA dyes without polar substituents is not influenced by solvent effects.[47] In contrast, the fluorescence of **MC** is known to show blueshifts with increasing polarity of the solvent.[48]

The fluorescence quantum yield (FQY) of **DHA-SP** in MeCN was determined to 0.37%. This is tenfold larger than that of the parent DHA (0.03%) in EtOH.[31] It should be noted that this more efficient fluorescence is a result of the new ICT state formed between DHA and SP and not just an increased fluorescence quantum yield of a locally excited DHA.

Fluorescence lifetimes (Table S4) of **DHA-SP** were measured in all solvent compositions and showed a large solvent dependency. For MeCN and DCM the decay is dominated by a very short lifetime component $\approx$200 ps, while in DCM:heptane the fast decay component is absent and $<\tau>\approx 1.5$ ns. In cyclohexane the lifetimes showed a dependency on emission wavelength, which indicates that both ICT and LE state may contribute. Radiative lifetimes (τ_0) were calculated based on the fluorescence quantum yields and average intensity weighted lifetimes $<\tau>$. These range from 20 ns in DCM to almost 500 ns in DCM:heptane (1:9), which highlights the low radiative rates of the ICT emission. The photophysical and switching properties of the **DHA-SP** dyad system are summarized in Figure 4 (bottom). Excitation with UV light (365 nm) can lead to the local excitation of the SP unit (**DHA-SP***) which may conduct to ring-opening of the spiropyran to give **DHA-MC**, selectively unachievable due to its further photoreaction (at 365 nm radiation) to the fully opened **VHF-MC**. **DHA-SP*** may also relax to the lower energy state **DHA*-SP**, locally excited at the DHA unit, which also can be obtained selectively at longer wavelength excitation (415 nm). In the more polar solvents, the **DHA*-SP** state is fast relaxing to an ICT state (as the formation of the ICT state is not detected in the lifetime measurements with a time resolution of $\approx$ 20 ps). The energy of the ICT state is highly polarity dependent, and it deactivates mainly non-radiatively to the ground state, though in competition with fluorescence (~0.5%) and ring-opening to **VHF-SP** (~5%).

Conclusions

In conclusion, a multiswitchable system has been obtained where one of the two switching units provides its intrinsic fluorescence as detection channel. Moreover, the design gave rise to an additional emission that apparently stems from the combination of structural units instead of being an intrinsic feature of the individual units. It was possible to access all eight theoretical states of the synthesized dyad **DHA-SP** selectively by light/heat and acid/base stimuli. These eight states, designated by binary numbers and by the directionality of the switching, are summarized with a 3D representation in Figure 5. Multiple switching paths featuring simultaneous, orthogonal, or path-dependent behavior in-between all eight states of the system were detected. The photoswitching of DHA to VHF, the ring-opening from SP to MC and *Z*/*E* isomerization from *Z*-MCH to *E*-MCH, as well as the protonation/deprotonation in between SP and *Z*-MCH, and MC and *E*-MCH, respectively, were successfully addressed and occurred independently from the switching state of the other switch in the dyad almost quantitatively. The photoswitching of the DHA/VHF couple and the acid/base switching of SP/*Z*-MCH were found to occur orthogonally and reversibly. The *Z*-MCH states ($<001>$ and $<101>$) converged unidirectionally to their *E*-MCH equivalents ($<011>$ and $<111>$). Thus, **DHA-SP** ($<000>$) and **DHA-*E*-**

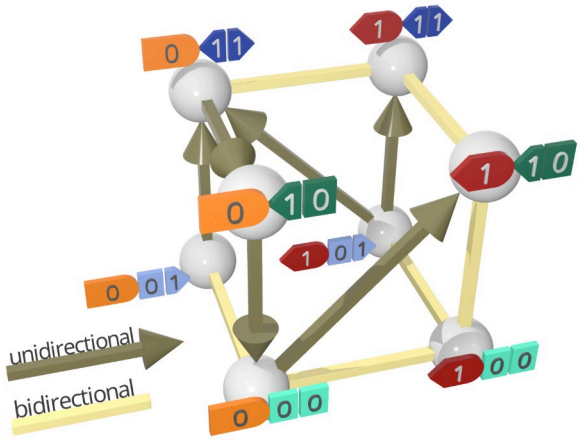

Figure 5. 3D representation of the switching pathways and logical coordinates of the accessible switching states of the dyad. The X-dimension represents DHA/VHF switching; the Y-dimension represents ring opening/closing of the SP/MC part; the Z-dimension represents protonation/deprotonation of the SP/MC part. The connections of the spheres show whether the transformation is unidirectional or bidirectional.

MCH (<011>) are the two thermally stable states of the system. In contrast, the two MC states, **DHA-MC** and **VHF-MC** (<010>, and <110>, respectively), were found to be relatively short-lived and could only be characterized by UV-vis absorption spectroscopy. Nevertheless, they functioned as crucial intermediates in the conversion in-between the longer lived states and proved the independent switchability of each switch. As next steps, it could be interesting to perform structural modifications aimed at enhancing the lifetimes of the **DHA-MC** and **VHF-MC** forms.

A remarkable fluorescence was detected for **DHA-SP** in comparison to the separate chromophores **SP** and **DHA**, which suggests the formation of a polar emissive ICT state after excitation. This emission appears to stem from the DHA moiety and was turned off when switching to VHF, as well as when switching the SP moiety to *Z*-MCH or *E*-MCH. We did, however, observe emission from the open MC and *E*-MCH moieties in **VHF-MC** (<110>) and **VHF-*E*-MCH** (<111>).

Thermal VHF-DHA relaxations were found to depend slightly on the neighboring unit, being faster when connected to an electron-withdrawing *E*-MCH unit than to an SP unit. For both MC isomers (**DHA-MC**/<010>, and **VHF-MC**/<110>), thermal MC-to-SP isomerization occurred much faster than thermal VHF-to-DHA isomerization, converting the isomers rapidly into the respective SP isomers. The MC-SP relaxations also showed a dependence on the neighboring unit, where the thermal half-life of **DHA-MC** is approx. twice as long as that of **VHF-MC**.

While the linear conjugation of the DHA and SP units lead to the solvatochromic fluorescence, both units retained their photoswitching properties. This is a striking difference to what has been observed for DHA-azobenzene dyads[49] (and in part for DHA-norbornadiene dyads[50]), where a cross-conjugated *meta*-phenylene connectivity was required for photoactivity. This "*meta*-rule" of photoactivity has also been established for the connection of azobenzene multimers.[51,52] The establishment of such "photoswitching design rules" for various dyads is crucial for future generations of multi-photochromic systems.

Acknowledgements

M.D. thanks the German Research Foundation (DFG) for a Research Fellowship (#441212186). M.C. thanks MIUR-Italy, "Progetto Dipartimenti di Eccellenza 2018–2022" allocated to the Department of Chemistry "Ugo Schiff".

Conflict of Interest

The authors declare no conflict of interest.

Data Availability Statement

The data that support the findings of this study are available in the supplementary material of this article.

Keywords: dihydroazulene · electrocyclic reactions · fluorescence · photochromism · spiropyran

[1] B. L. Feringa, W. R. Browne, Eds., *Molecular Switches*, Wiley-VCH, Weinheim, Germany, **2011**.
[2] B. L. Feringa, *Angew. Chem. Int. Ed.* **2017**, *56*, 11060–11078; *Angew. Chem.* **2017**, *129*, 11206-11226.
[3] R. Herges, *Chem. Sci.* **2020**, *11*, 9048–9055.
[4] I. Aprahamian, *ACS Cent. Sci.* **2020**, *6*, 347–358.
[5] Z. Li, C. Y. Gao, D. Su, C. Jia, X. Guo, *ACS Materials Lett.* **2021**, *3*, 1484–1502.
[6] E. Moulin, L. Faour, C. C. Carmona-Vargas, N. Giuseppone, *Adv. Mater.* **2020**, *32*, 1906036.
[7] I. Yildiz, E. Deniz, F. M. Raymo, *Chem. Soc. Rev.* **2009**, *38*, 1859–1867.
[8] R. Klajn, *Chem. Soc. Rev.* **2014**, *43*, 148–184.
[9] Z. L. Pianowski, *Chem. Eur. J.* **2019**, *25*, 5128–5144.
[10] A. Goulet-Hanssens, F. Eisenreich, S. Hecht, *Adv. Mater.* **2020**, *32*, 1905966.
[11] Y. Zheng, Y. Meana, M. M. A. Mazza, J. D. Baker, P. J. Minnett, F. M. Raymo, *J. Am. Chem. Soc.* **2022**, *144*, 4759–4763.
[12] X. Huang, T. Li, *J. Mater. Chem. C* **2020**, *8*, 821–848.
[13] G. Xu, S. Li, C. Liu, S. Wu, *Chem. Asian J.* **2020**, *15*, 547–554.
[14] L. Dong, Y. Feng, L. Wang, W. Feng, *Chem. Soc. Rev.* **2018**, *47*, 7339–7368.
[15] J. Orrego-Hernández, A. Dreos, K. Moth-Poulsen, *Acc. Chem. Res.* **2020**, *53*, 1478–1487.
[16] M. B. Nielsen, N. Ree, K. V. Mikkelsen, M. Cacciarini, *Russ. Chem. Rev.* **2020**, *89*, 573–586.
[17] R. Ballardini, V. Balzani, J. Becher, A. D. Fabio, M. T. Gandolfi, G. Mattersteig, M. B. Nielsen, F. M. Raymo, S. J. Rowan, J. F. Stoddart, A. J. P. White, D. J. Williams, *J. Org. Chem.* **2000**, *65*, 4120–4126.
[18] L. Casimiro, S. Maisonneuve, P. Retailleau, S. Silvi, J. Xie, R. Métivier, *Chem. Eur. J.* **2020**, *26*, 14341–14350.
[19] A. Gerwien, B. Jehle, M. Irmler, P. Mayer, H. Dube, *J. Am. Chem. Soc.* **2022**, *144*, 3029–3038.
[20] M. Irie, T. Fukaminato, K. Matsuda, S. Kobatake, *Chem. Rev.* **2014**, *114*, 12174–12277.
[21] M. Han, R. Michel, B. He, Y.-S. Chen, D. Stalke, M. John, G. H. Clever, *Angew. Chem. Int. Ed.* **2013**, *52*, 1319–1323; *Angew. Chem.* **2013**, *125*, 1358–1362.
[22] F. Zhao, L. Grubert, S. Hecht, D. Bléger, *Chem. Commun.* **2017**, *53*, 3323–3326.
[23] A. H. Heindl, J. Becker, H. A. Wegner, *Chem. Sci.* **2019**, *10*, 7418–7425.
[24] C. Guerrin, Y. Aidibi, L. Sanguinet, P. Leriche, S. Aloise, M. Orio, S. Delbaere, *J. Am. Chem. Soc.* **2019**, *141*, 19151–19160.
[25] L. Gobbi, P. Seiler, F. Diederich, *Angew. Chem. Int. Ed.* **1999**, *38*, 674–678; *Angew. Chem.* **1999**, *111*, 737–740.
[26] J. Andréasson, U. Pischel, S. D. Straight, T. A. Moore, A. L. Moore, D. Gust, *J. Am. Chem. Soc.* **2011**, *133*, 11641–11648.
[27] M. Bälter, S. Li, J. R. Nilsson, J. Andréasson, U. Pischel, *J. Am. Chem. Soc.* **2013**, *135*, 10230–10233.
[28] A. Vlasceanu, M. Koerstz, A. B. Skov, K. V. Mikkelsen, M. B. Nielsen, *Angew. Chem. Int. Ed.* **2018**, *57*, 6069–6072; *Angew. Chem.* **2018**, *130*, 6177–6180.
[29] A. Fihey, A. Perrier, W. R. Browne, D. Jacquemin, *Chem. Soc. Rev.* **2015**, *44*, 3719–3759.
[30] G. Szalóki, G. Sevez, J. Berthet, J.-L. Pozzo, S. Delbaere, *J. Am. Chem. Soc.* **2014**, *136*, 13510–13513.
[31] H. Goerner, C. Fischer, S. Gierisch, J. Daub, *J. Phys. Chem.* **1993**, *97*, 4110–4117.
[32] S. L. Broman, S. L. Brand, C. R. Parker, M. Å Petersen, C. G. Tortzen, A. Kadziola, K. Kilså, M. B. Nielsen, *Arkivoc* **2011**, *2011*, 51–67.
[33] L. Kortekaas, W. R. Browne, *Chem. Soc. Rev.* **2019**, *48*, 3406–3424.
[34] L. Kortekaas, J. Chen, D. Jacquemin, W. R. Browne, *J. Phys. Chem. B* **2018**, *122*, 6423–6430.
[35] C. L. Fleming, S. Li, M. Grøtli, J. Andréasson, *J. Am. Chem. Soc.* **2018**, *140*, 14069–14072.
[36] C. Berton, D. M. Busiello, S. Zamuner, E. Solari, R. Scopelliti, F. Fadaei-Tirani, K. Severin, C. Pezzato, *Chem. Sci.* **2020**, *11*, 8457–8468.
[37] L. Gobbi, P. Seiler, F. Diederich, V. Gramlich, C. Boudon, J.-P. Gisselbrecht, M. Gross, *Helv. Chim. Acta* **2001**, *84*, 743–777.
[38] M. Schulz-Senft, P. J. Gates, F. D. Sönnichsen, A. Staubitz, *Dyes Pigm.* **2017**, *136*, 292–301.

[39] UV-Vis spectroscopic analysis of the relaxation of **VHF-*E*-MCH** to **DHA-*E*-MCH** showed a second reaction appearing after ca. 4 h; the ^{1}H-NMR spectrum also revealed some degradation. ^{1}H-NMR spectroscopic analysis, however, confirmed a clean VHF/DHA isomerization within the detection limits during the first 4 h.
[40] S. L. Broman, M. Jevric, M. B. Nielsen, *Chem. Eur. J.* **2013**, *19*, 9542–9548.
[41] A. K. Chibisov, H. Görner, *J. Photochem. Photobiol. A* **1997**, *105*, 261–267.
[42] H. Görner, *Phys. Chem. Chem. Phys.* **2001**, *3*, 416–423.
[43] V. A. Barachevsky, *J. Fluoresc.* **2000**, *10*, 185–185.
[44] A. K. Chibisov, H. Görner, *J. Phys. Chem. A* **1997**, *101*, 4305–4312.
[45] Z. R. Grabowski, K. Rotkiewicz, W. Rettig, *Chem. Rev.* **2003**, *103*, 3899–4032.
[46] M. Szyszkowska, I. Bylińska, W. Wiczk, *J. Photochem. Photobiol. A* **2016**, *326*, 76–88.
[47] T. Mrozek, H. Görner, J. Daub, *Chem. Eur. J.* **2001**, *7*, 1028–1040.
[48] R. Rosario, D. Gust, M. Hayes, J. Springer, A. A. Garcia, *Langmuir* **2003**, *19*, 8801–8806.
[49] A. Mengots, A. Erbs Hillers-Bendtsen, S. Doria, F. Ørsted Kjeldal, N. Machholdt Høyer, A. Ugleholdt Petersen, K. V. Mikkelsen, M. Di Donato, M. Cacciarini, M. B. Nielsen, *Chem. Eur. J.* **2021**, *27*, 12437–12446.
[50] M. D. Kilde, M. Mansø, N. Ree, A. U. Petersen, K. Moth-Poulsen, K. V. Mikkelsen, M. B. Nielsen, *Org. Biomol. Chem.* **2019**, *17*, 7735–7746.
[51] C. Slavov, C. Yang, L. Schweighauser, C. Boumrifak, A. Dreuw, H. A. Wegner, J. Wachtveitl, *Phys. Chem. Chem. Phys.* **2016**, *18*, 14795–14804.
[52] C. Yang, C. Slavov, H. A. Wegner, J. Wachtveitl, A. Dreuw, *Chem. Sci.* **2018**, *9*, 8665–8672.

Manuscript received: June 1, 2022
Accepted manuscript online: June 13, 2022
Version of record online: July 27, 2022